ISSN 0026-2617, Microbiology, 2013, Vol. 82, No. 6, pp. 809–814. © Pleiades Publishing, Ltd., 2013.
Original Russian Text © D.N. Matorin, D.A. Todorenko, N.Kh. Seifullina, B.K. Zayadan, A.B. Rubin, 2014, published in Mikrobiologiya, 2014, Vol. 83, No. 1, pp. 33–40.

EXPERIMENTAL ARTICLES

Effect of Silver Nanoparticles on the Parameters of Chlorophyll Fluorescence and P_{700} Reaction in the Green Alga *Chlamydomonas reinhardtii*

D. N. Matorin[a, 1], D. A. Todorenko[a], N. Kh. Seifullina[a], B. K. Zayadan[b], and A. B. Rubin[a]

[a] *Faculty of Biology, Moscow State University, Russia*

[b] *Al-Farabi Kazakhstan National University, Alma-Aty, Kazakhstan*

Received June 18, 2013

Abstract—Acute toxicity of silver nanoparticle (AgNP) for photosynthesis in *Chlamydomonas reinhardtii* was studied using an M-PEA2 fluorimeter. Analysis of the fluorescence induction curves in the presence of AgNP at low concentrations revealed inhibited electron transport on the PS2 photosystem and increased content of Q_B-nonreducing centers. No direct effect of AgNP on the reactions of P_{700} oxidation in PS1 was found, while the energization of the photosynthetic membranes was affected. Investigation of the parameters of the prompt and delayed fluorescence is proposed as a method for early detection of AgNP in the environment.

Keywords: *Chlamydomonas reinhardtii*, silver nanoparticles, chlorophyll fluorescence, photosynthesis, ecology

DOI: 10.1134/S002626171401010X

Silver-containing materials, including metallic silver nanoparticles, are presently widely used for manufacturing a number of products. These include fabrics, air filters, cosmetics, toothpaste, childcare products, vacuum cleaners, and washing machines [1]. Numerous silver-containing medicinal preparations that possess antimicrobial properties due to the presence of silver ions have entered the market [2].

For a long period of time, it was considered an ascertained fact that Ag^+ ions, rather than metallic silver, exhibit therapeutic effects. However, the mechanism of action of silver nanoparticles on various biological objects is still unclear and requires further investigation [2]. Toxicity of silver ions against algae has been studied in a number of works [5, 6]. The toxic effects of AgNP on freshwater algae *Chlamydomonas reinhardtii* was demonstrated [7, 8]. It was found that AgNP may inhibit photosynthesis in environmental phytoplankton, which is the basis of the productivity of aquatic ecosystems [4].

The probability of AgNP arriving into aquatic ecosystems and becoming a source of dissolved silver, which may exert toxic effects on water organisms, is high [3, 4].

In toxicological experiments on microalgae, fluorescence methods are used, making it possible to monitor the photosynthesis processes and providing detailed information on the primary defects of cell metabolism, mainly at the membrane level [4, 9, 10]. Importantly, these methods provide information on the state of natural phytoplankton in real time. Due to emission of fluorescence quanta, chlorophyll of the algal photosynthetic membranes may act as a natural indicator of photosynthetic activity. Measurement of the ratio between the fluorescence intensity under the photosynthesis-saturating illumination (F_m) and under conditions inducing no changes in the state of the photosynthetic apparatus (F_o) (low light intensity) makes it possible to determine the maximum efficiency of the PS2 processes, which is equal to $(F_m - F_o)/F_m = F_v/F_m$. The F_v/F_m value presents a dimensionless energetic characteristics of photosynthesis, similar to the coefficient of efficiency and independent of the species-specific features of an organisms.

Methods of fluorescence induction curve detection with high time resolution (starting from 10 μs) under excitation with intense light have been recently used to assess the work of photosynthetic apparatus in higher plants and algae cultures [11–15]. Measurement of fluorescence induction curves with high resolution takes several seconds and is performed on the PAM or PEA type equipment. The M-PEA2 instrument makes it possible to measure the changes in P_{700} (PS1 pigment) absorption alongside registration of fluorescence. In other words, this instrument allows simultaneous registration of separate reactions in PS1 and PS2 [11, 12]. Moreover, it monitors induction changes in delayed fluorescence, which provides information

[1] Corresponding author; e-mail: matorin@biophys.msu.ru

Abbreviations used: AgNP, silver nanoparticles; PS2, photosystem 2; RC, reaction center; Q_A and Q_B, primary and secondary quinone electron acceptors; PQ, plastoquinone; O, J, I, and P, intermediate stages of light-induced fluorescence curve; DF, delayed fluorescence; P_{700}, pigment of the RC in PS1.

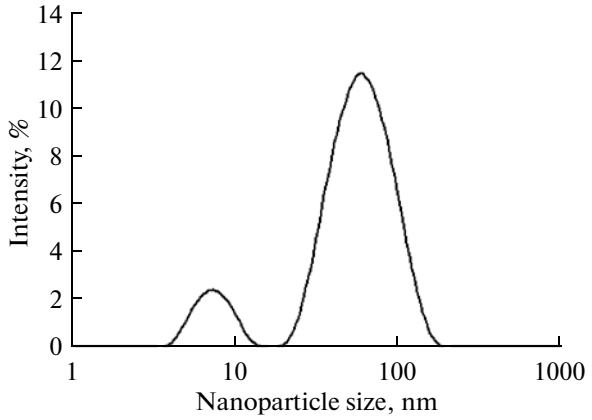

Fig. 1. Histogram of silver nanoparticle size distribution measured on a Zetasizer Nano ZS.

on kinetics of the proton electrochemical gradient across the photosynthetic membrane [4].

In the work, we used an M-PEA2 fluorimeter to study the processes in PS1 and PS2 and the proton electrochemical gradient on a thylakoid membrane of the alga *Chlamydomonas reinhardtii* after treatment with silver nanoparticles at concentrations inducing changes in the F_v/F_m ratio.

The goal of the present work was to study the possibility of application of analysis of chlorophyll prompt fluorescence kinetics to assess the state of the algal photosynthetic apparatus at early stages of toxic action of silver nanoparticles.

MATERIALS AND METHODS

Green algae *Chlamydomonas reinhardtii* Dang c137+ grown under phototrophic conditions in Tris–acetate–phosphate medium were chosen as the subject of the study. The algae were cultured by accumulation under illumination with 30 μE/m^2 light at 18–20°C. Initial density of the culture was 300×10^3 cells/mL. Stationary-phase cultures were used in the experiments. Algal cells were counted microscopically in a Goryaev chamber.

Fluorescence measurements of the algae were performed on an M-PEA2 (HansaTech, United Kingdom) instrument that allows simultaneous registration of prompt and delayed fluorescence induction, as well as of the changes in P_{700} absorbance at 820 nm with high time resolution (starting from 0.01 ms). Prompt and delayed fluorescence were registered upon alteration of periods of actinic illumination (627 nm, 1200 μE/(m^2 s)) and darkness. Prior to the measurements, the cells were concentrated on a membrane filter, and the filtered sample was placed in a measurement cell and incubated in the darkness for 10 min. The F_v/F_m values were measured directly in the algal culture on an Aqua-Pen fluorimeter (Photon Systems Instruments, Czech Republic).

A sample of silver nanoparticles from Sigma Aldrich was used in the experiments. Particle size was determined in a purified suspension in water using dynamic light scattering on a Zetasizer Nano ZS (Malvern, Great Britain). A chemical preparation of silver nitrate ($AgNO_3$) was used for comparison.

All measurements were performed at least in five repeats. The figures present data of at least three repeated experiments.

RESULTS

Figure 1 presents a histogram of silver nanoparticle size distribution. In 10% water solution, the average diameter of the major group of particles was about 80 ± 13 nm.

Fluorescence measurements of *C. reinhardtii* cultures confirmed that the photosynthetic apparatus of this alga was a sensitive target for silver nanoparticles. After a 24-h incubation with silver nanoparticles (2×10^{-6} M), PS2 activity decreased. At concentration of 2×10^{-5} M, AgNP induced a decrease in the F_v/F_m value from 0.71 to 0.66 (table). Silver nitrate was also found to induce a decrease in F_v/F_m to the value of 0.64 at the same concentration (10^{-5} M).

For more detailed investigation of the effect of AgNP on photosynthetic activity of the algal cells, parameters of prompt and delayed fluorescence, as well as P_{700} absorption, were measured on M-PEA2 (Fig. 2). These studies were important not only to understand the basic mechanisms of AgNP effect on PS1 and PS2 functioning and the processes of energization the photosynthetic membranes, but also for the possible application of various fluorescence parameters in biomonitoring studies on toxicological effects of silver nanoparticles in aqueous systems.

Figure 2 presents kinetic curves of fluorescence induction after switching the light on normalized against the O level. In the control cells, the shape of the fluorescence curve corresponded to that described in the literature [11–15]. Usually, several components are observed in the kinetics of fluorescence induction in response to high-intensity illumination, namely, the O–J–I–P transitions. The initial level O corresponds to chlorophyll fluorescence intensity under open RCs of PS2 (F_o) when all Q_A are oxidized. The time period required to reach this level is up to 50 μs. The O–J phase is caused by light-induced reduction of Q_A, while the subsequent phases reflect mainly further accumulation of reduced Q_A^-, caused by a decrease in its re-oxidation rate as a result of reduction of Q_B acceptors and the pool of quinones.

It should be noted that measurements on an M-PEA2 fluorimeter were performed using the cells that have been preliminarily filtered through a membrane filter. Control measurements performed on an Aqua-Pen demonstrated matching between its data and the curves obtained with M-PEA2 (Figs. 2 and 3).

Parameters of OJIP kinetics of fluorescence induction measured in *Chlamydomonas reinhardtii* cells after 24 h incubation with AgNP at various concentrations. The kinetic parameters of fluorescence induction were measured on M-PEA2 under illumination of 1000 μE/(m^2 s)

JIP test parameters		Control	AgNP 2×10^{-6} M	AgNP 2×10^{-5} M
F_v/F_m	Maximum quantum yield of charge separation in PS2	0.71	0.69	0.66
V_J	Relative amplitude of the O–J phase	0.39	0.41	0.43
V_I	Relative amplitude of the J–I phase	0.67	0.68	0.68
M_O	Initial slope of the O–J fluorescence phase	0.86	0.90	0.93
S_M	Area between the fluorescence kinetic curve (O–J–I–P) and the level of F_m normalized against the F_v value	19.11	19.78	20.9
ABS/RC	Average value of absorbed photon flows in PS2 RC (or apparent size of the active antenna in PS2)	3.12	3.17	3.29
q_E	Capacity for pH-induced non-photochemical fluorescence quenching	0.41	0.40	0.32
q_{PQ}	Capacity of the quinone pool for fluorescence quenching	0.33	0.32	0.32

This similarity indicates that the procedure of sample enrichment on filters that used in the present work did not affect the physiological state of the cells.

Treatment with AgNP resulted in changed shape of the O–J–I–P curve and in decreased contribution of the J–I–P photochemical phase, indicating impaired electron flow from PS2 to the quinone pool.

To quantitatively analyze the characteristics of the primary processes of photosynthesis on the basis of O–J–I–P kinetic curve parameters, the so-called JIP-test [4, 11] was used. The JIP-test operates the following parameters of the fluorescence induction kinetic curve: (a) fluorescence intensity at 50 μs (F_o), 300 μs ($F_{300\ \mu s}$), 2 ms (F_J), 30 ms (F_I), 6 s ($F_{6\,s}$), and F_P (F_m, the maximum fluorescence yield); (b) time to reach the maximum fluorescence (tF_m), and (c) area under the kinetic curve below the F_m level.

These characteristics were used to calculate the following parameters presented in the table: (1) maximum efficiency of PS2 ($F_v/F_m = F_m - F_o/F_m$); (2) relative amplitude of the O–J phase ($V_j = (F_j - F_o)/F_v$), which reflects the share of non-Q_B-reducing PS2 which lack the contact between the two consecutive PS2 acceptors, Q_A and Q_B; (3) relative amplitude of the J–I phase ($V_I = (F_I - F_J)/F_v$); (4) M_O parameter ($M_O = 4 \times (F_{300\,\mu s} - F_o)/F_v$), which reflects the initial slope of the induction curve; M_O value is proportional to the rate of Q_A reduction under conditions when Q_B and the pool of plastoquinones are mainly in the oxidized state; (5) $S_M = (\text{Area})/F_v$, normalized value of the area between the OJIP curve and F_m value reflecting the total rounds of PS2 during the OJIP phase of growth of the fluorescence yield; (6) ABS/RC – M_O $(1/F_v/F_m)$ $(1/V_J)$, average value of absorbed photon streams in RC of PS2 (observed size of the active PS2 antenna); (7) capacity for pH-induced non-photochemical fluorescence quenching ($q_E = (F_m - F_{6\,s})/F_v$); and (8) capability of the quinone pool to quench fluorescence $q_{PQ} = (F_m - F_I)/F_v$.

Many parameters of the JIP test are mutually dependent; that is, change in some of them leads to changes in the others. Independent parameters (V_J and M_O) derived form the analysis of the O–J phase provide the information on Q_A reduction. From the V_I and S_M parameters, it is possible to derive information on further accumulation of reduced Q_A^-, which occurs due to reduction of Q_B and the quinone pool.

It is assumed that the O–J phase of fluorescence induction reflects accumulation of Q_A^- in both Q_B^--reducing and non-reducing PS2 [11, 13]. The hypothesis is supported by the fact that diuron, which inhibits electron transport between Q_A and Q_B, leads to fast growth of fluorescence to the maximum level within 2 ms, corresponding to the appearance of the J peak in the control. Analysis demonstrated that AgNP treatment resulted in an increased number of non-Q_B-reducing centers in PS2 incapable of reduction of the quinone pool. This was supported by a number of other parameters

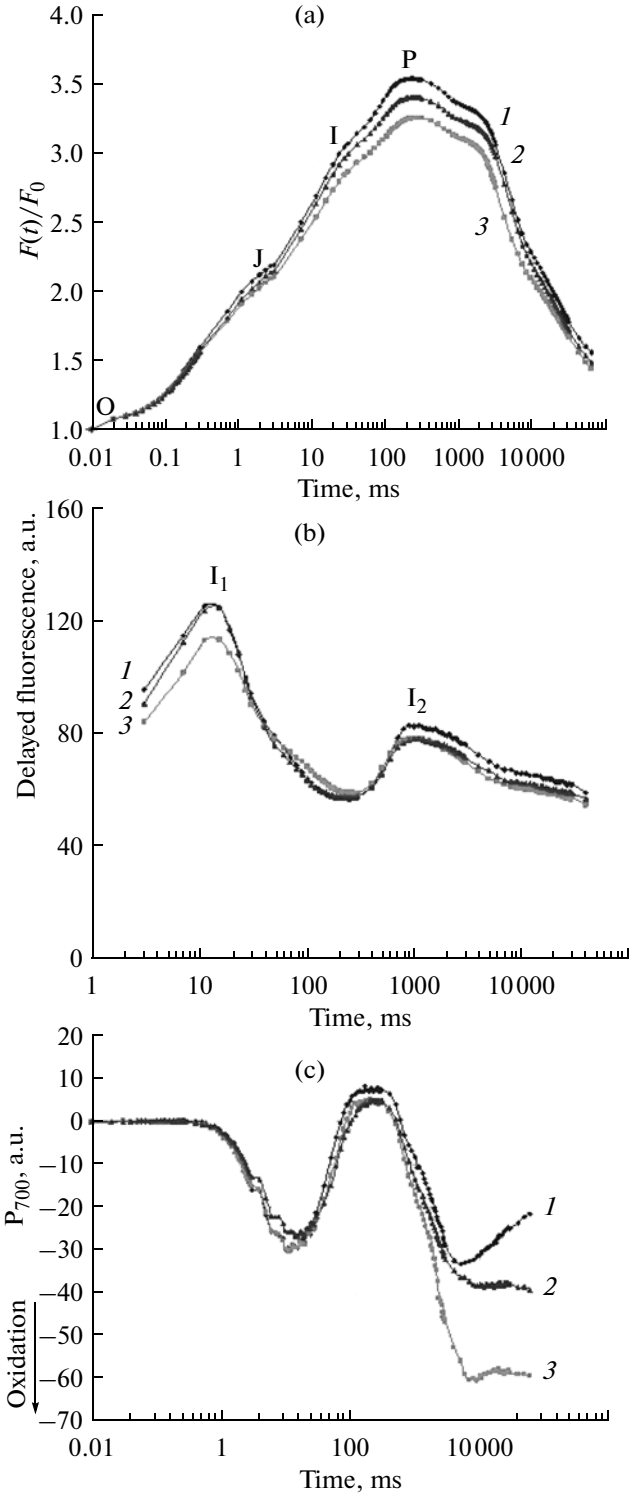

Fig. 2. Induction curves of prompt (a) and delayed (b) fluorescence and change in absorption at 820 nm (c) after turning on the light in the culture of *Chlamydomonas reinhardtii* after 24 h of incubation with AgNP at various concentrations: control (*1*), 2×10^{-6} M (*2*), and 2×10^{-5} M (*3*). Intensity of the light was 1000 μE/(m^2 s). Incubation with AgNP for 24 h. Simultaneous measurements of all the parameters on M-PEA2.

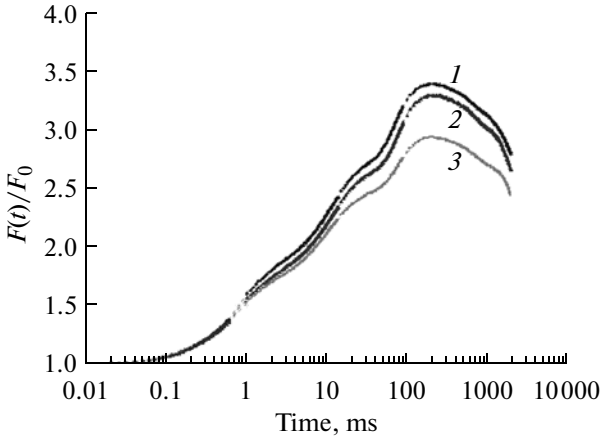

Fig. 3. Induction curves of prompt fluorescence of chlorophyll after turning on the light in a culture of *Chlamydomonas reinhardtii* after 24 h of incubation with AgNP at various concentrations: control (*1*), 2×10^{-6} M (*2*), and 2×10^{-5} M (*3*). Intensity of the light was 1000 μE/(m^2 s). Incubation with AgNP for 24 h. Simultaneous measurements of all the parameters on Aqua-Pen.

(table). Accordingly, values of the parameters M_O, which reflect the initial slope of the induction growth curve, as well as S_M, increased. Total flow of photons consumed by the pigments of the PS2 antenna normalized against RC (ABS/RC) increased in the cultures treated with AgNP, if compared to the control values. At the same time, the relative amplitude of the J–I phase (V_I) practically did not change.

Prompt fluorescence induction curves also demonstrated the suppression of fluorescence decay after reaching the maximum due to ΔpH-dependent nonphotochemical quenching ($q_E = (F_m - F_{6\,s})/F_v$). The value of this parameter decreased in the presence of AgNP, which evidences a decrease in the membrane energization. At the same time, the ability of the quinone pool to quench fluorescence $q_{PQ} = (F_m - F_I)/F_v$ in algae treated with AgNP did not change.

Simultaneous registration of ΔA820 kinetic curve on M-PEA2 showed that light applied to a darkness-adapted subject induced initial oxidation of P_{700} (with the maximum P_{700}^+ accumulation at $t \approx 30$ ms), which was followed by reduction of P_{700} (Fig. 2). Signals of fluorescence reflecting Q_A reduction and processes of P_{700} reduction reached a plateau at approximately the same time. Accumulation of reduced forms of P_{700} and Q_A in parallel reflected reduction of carriers over the whole region of ETC between the photosystems due to the lack of flow-out of electrons from the acceptor part of PS1 under conditions when ferredoxin–NADP reductase (FNR) was inactivated due to incubation in the dark [12, 14]. Prolonged illumination (~10 s) resulted in a second wave of P_{700} oxidation, which is

explained by the electron flow-out from the PS1 upon activation of FNR and the Calvin cycle enzymes.

In the presence of AgNP, the PS1 RC pigment, P_{700}, was capable of processes of oxidation upon turning on the light (Fig. 2). However, in algae treated with AgNP, decrease in the rate of reduction from PS2 was observed due to inhibition of electron transport. These changes were especially noticeable in the time interval >10 s and were in agreement with an increase in non-Q_B-reducing RC of PS2.

Delayed fluorescence is known to be one of the methods used to monitor the changes in proton gradient across the cell membrane [4]. The phenomenon of delayed fluorescence refers to the weak, slowly attenuating red glow emitted by chlorophyll in photosynthesizing cells upon excitation with light [4, 15]. This glow rises after termination of the prompt fluorescence (PF) at the expense of the energy exerted in the process of reactions of the primary photoproducts in the PS2 RC. The difference between the prompt and delayed fluorescence stems from the nature of excitation of the emitting chlorophyll molecule. PF is linked to the processes of deactivation of chlorophyll excitation before separation of the charges in RC, while DF rises after the primary act of photosynthesis and the energy appears as a result of reverse recombination of separated charges in the reaction center of PS2. PF is a purely photophysical process and is caused by emission of a fraction of the energy adsorbed by the antenna chlorophyll which did not migrate to the reaction center. DF is in tight connection with the photochemical reactions occurring in the PS2 RC. The peak of the DF curve in the millisecond range (I_1) matches the phase of J–I increase of the fast fluorescence induction curve (Fig. 2). Formation of I_1 may be caused by accumulation of certain redox states responsible for recombination of the charges and emission of DF quanta (that is, emitting states), as well as for the increase in DF due to the membrane electrical potential thus formed. The presence of the second DF peak, I_2, in the range of seconds, is associated with the light-induced formation of the proton transmembrane gradient that increases the constant of rate of emission transitions in the RC of PS2. These mechanisms are reviewed in many works (see [4]).

In the presence of AgNP (at relatively low concentrations), peaks of delayed fluorescence curve in the ranges of 20–50 ms and around 1 s decreased, which evidenced a decrease in the electrical (potential) and chemical constituents of the electrochemical proton gradient.

Thus, simultaneous registration of fast and delayed fluorescence induction, together with changes in P_{700}, made it possible to monitor the individual reactions of accumulation of reduced carriers between the photosystems, switching on of PS1, and kinetics of electrochemical proton gradient on a thylakoid membrane in the presence of AgNP.

DISCUSSION

Microalgae using solar energy for synthesis of organic matter act as the main source of energy in aquatic ecosystems and as food for other organisms. Therefore, phytoplankton may be the first stage/barrier in accumulation of nanoparticles in the food chains of aquatic ecosystems. Owing to their wide spectrum of applications, the probability of silver nanoparticles (AgNP) may arrive into aquatic ecosystems is high [3, 4].

Our results confirmed toxicity of low concentrations (10^{-6}–10^{-5} M) of silver nanoparticles for a microalgal culture. Simultaneous studies performed on an M-PEA2 revealed the specific features of nanoparticle (AgNP) effect on reactions in PS2 and the absence of direct effect on reactions of oxidation of the PS1 pigment P_{700}. Analysis of fluorescence induction curves demonstrated the inhibition of electron transport in PS2 and an increase in the share of non-Q_B-reducing centers. Moreover, analysis of induction curves for delayed fluorescence revealed the effect of nanoparticles on the processes of energization of the cellular photosynthetic membranes.

Despite the fact that AgNP toxicity for bacteria was studied in a number of works [16–18], the mechanism of this effect is not clear yet. It is assumed that the toxic effect of AgNP may be associated with the damage of the cell membrane, oxidative stress, or interaction of Ag^+ with proteins and enzymes. Besides, the question on whether the toxic effect on microorganisms is specific for nanoparticles in general, or if it is the result of the action of silver ions, remains unclear.

In our experiments, no considerable difference was observed between silver in the form of nanoparticles and silver nitrate. This effect agrees with abundant literature data, since the release of metal ions from nanoparticles and the complexes they form may be the major factors of environmental toxicity of nanoparticles. Indeed, it has been demonstrated in vitro in cell cultures that the solubility of nanoparticles of metal oxides (including TiO_2 and ZnO) affected their cytotoxicity considerably [19]. It was shown for the alga *Pseudokirchneriella subcapitata* that toxicity of nanoparticles and large ZnO particles may be exclusively associated with dissolved Zn. The results obtained in work [20] also demonstrated that toxicity of CuO and ZnO against bacteria and a crustacean *Thamnocephalus platyurus* was mainly associated with the bioavailability of Cu and Zn ions, in spite of low solubility of CuO and ZnO in water [21]. Similar data for the effect of CuO and ZnO nanoparticles on the alga *Pseudokirchneriella subcapitata* and *Selenastrum capricornutum* were presented in work [22]. In work [8], the authors tried to resolve the issue by adding cysteine, a strong ligand of Ag^+. It was found that cysteine removed the inhibitory effect of both AgNP and Ag^+ on photosynthesis in algae. This allowed the authors to conclude that the presence of Ag^+ in suspension of AgNP cannot explain their toxicity completely. These

results indicate interaction between the particles and the algae, which enhances toxicity of AgNP via Ag^+. A hypothesis was proposed that toxicity of the particles is due to the release of silver ions formed in the presence of algae.

Our studies showed that changes in prompt and delayed fluorescence induction curves are among the first parameters of algal response to the introduction of nanoparticles in the medium. These parameters may be efficiently used for diagnostics of effect of nanomaterials on the algae, as well as for rapid detection of the presence of nanomaterials in the aquatic environments.

ACKNOWLEDGMENTS

The authors are thankful to V.A. Osipov for his help with the measurements.

The work was supported by the Russian Foundation for Basic Research (project no. 13-04-01853) and the Federal Target Program (project no. 14.512. 11.0097).

REFERENCES

1. Lee, H.Y., Park, H.K., Lee, Y.M., and Park, S.B., A practical procedure for producing silver nanocoated fabric and its antibacterial evaluation for biomedical applications, *Chem. Commun.*, 2007, vol. 28, pp. 2959–2961.
2. Choi, O., Deng, K.K., Kim, N.J., Ross, L., Jr., and Surampalli, R.Y., The inhibitory effects of silver nanoparticles, silver ions, and silver chloride colloids on microbial growth, *Water Res.*, 2008, vol. 42, pp. 3066–3074.
3. Wiesner, M.R., Lowry, G.V., Alvarez, P., Dionysiou, D., and Biswas, P., Assessing the risks of manufactured nanomaterials, *Environ. Sci. Technol.*, 2006, vol. 40, pp. 4336–4345.
4. Matorin, D.N. and Rubin, A.B., *Fluorestsentsii khlorofilla vysshikh rastenii i vodoroslei* (Chlorophyll Fluorescence in Algae and Higher Plants), Moscow–Izhevsk: IKI-RKhD, 2012.
5. Hiriart-Baer, V.P., Lee, D.Y., and Campbell, P.G., Toxicity of silver to two freshwater algae *Chlamydomonas reinhardtii* and *Pseudokirchneriella subcapitata* grown under continuous culture conditions: Influence of thiosulphate, *Aquat. Toxicol.*, 2006, vol. 78, pp. 136–148.
6. Dmitrieva, A.G., Boichuk, T.V., and Filenko, O.F., Population heterogeneity in *Scenedesmus quadricauda* under different modes of silver intoxication, *Ekol. Pribory Sistemy*, 2007, no. 3, pp. 42–45.
7. Oukarroum, A., Perreault, F., Bras, S., and Popovic, R., Inhibitory effects of silver nanoparticles in two green algae, *Chlorella vulgaris* and *Dunaliella tertiolecta, Ecotoxicol. Environ. Safety*, 2012, vol. 78, pp. 80–85.
8. Navarro, E., Piccapietra, F., Wagner, B., Kogi, R., Odzak, N., Sigg, L., and Behra, R., Toxicity of silver nanoparticles to *Chlamydomonas reinhardtii, Environ. Sci. Technol.*, 2008, vol. 42, pp. 8959–8964.
9. Matorin, D.N., Karateeva, A.V., Osipov, V.A., Lukashev, E.P., Seifullina, N.Kh., and Rubin A.B., Influence of carbon nanotubes on chlorophyll fluorescence parameters of green algae *Chlamydomonas reinhardtii, Nanotechnologies in Russia*, 2010, nos. 5–6, pp. 320–327.
10. Matorin, D.N., Osipov, V.A., Seifullina, N.Kh., Venediktov, P.S., and Rubin, A.B., Increasing toxic effect of methylmercury on *Chlorella vulgaris* under high light and cold stress conditions, *Microbiology* (Moscow), 2009, vol. 78, no. 3, pp. 321–327.
11. Strasser, R.J., Tsimilli-Michael, M., Qiang, S., and Goltsev, V., Simultaneous in vivo recording of prompt and delayed fluorescence and 820-nm reflection changes during drying and after rehydration of the resurrection plant *Haberlea rhodopensis, Biochim. Biophys. Acta*, 2010, vol. 1797, nos. 6–7, pp. 1313–1326.
12. Bulychev, A.A., Osipov, V.A., Matorin, D.N., and Vredenberg, W.J., Effects of far-red light on fluorescence induction in infiltrated pea leaves under diminished ΔpH and $\Delta\varphi$ components of the proton motive force, *J. Bioenerg. Biomembr.*, 2013, vol. 45, no. 1, pp. 37–45.
13. Antal, T.K., Osipov, V.A., Matorin, D.N., and Rubin, A.B., Membrane potential is involved in regulation of photosynthetic reactions in the marine diatom *Thalassiosira weissflogii, J. Photochem. Photobiol., Ser. B: Biol.*, 2011, vol. 102, pp. 169–173.
14. Bulychev, A.A., Induction changes in photosystem I and II in plant leaves upon modulation of membrane ion transport, *Biochemistry* (Moscow) *Suppl. Ser. A: Membr. Cell Biol.*, 2011, vol. 5, no. 4, pp. 335–342.
15. Goltsev, V., Zaharieva, I., Chernev, P., and Strasser, R.J., Delayed fluorescence in photosynthesis, *Photosynth. Res.*, 2009, vol. 101, pp. 217–232.
16. Kim, J.S., Kuk, E., Yu, K.N., Kim, J.H., Park, S.J., Lee, H.J., Kim, S.H., Park, Y.K., Park, Y.H., Hwang, C.Y., Kim, Y.K., Lee, Y.S., Jeong, D.H., and Cho, M.H., Antimicrobial effects of silver nanoparticles, *Nanomed. Nanotechnol. Biol. Med.*, 2007, vol. 3, pp. 95–101.
17. Pal, S., Tak, Y.K., and Song, J.M., Does the antibacterial activity of silver nanoparticles depend on the shape of the nanoparticle? A study of the gram-negative bacterium *Escherichia coli, Appl. Environ. Microbiol.*, 2007, vol. 73, pp. 1712–1720.
18. Yamanaka, M. Hara, K., and Kudo, J., Bactericidal actions of a silver ion solution on *Escherichia coli*, studied by energy-filtering transmission electron microscopy and proteomic analysis, *Appl. Environ. Microbiol.*, 2005, vol. 71, pp. 7589–7593.
19. Brunner, T.J., Wick, P., Manser, P., Spohn, P., Grass, R.N., Limbach, L.K., Bruinink, A., and Stark, W.J., In vitro cytotoxicity of oxide nanoparticles: comparison to asbestos, silica, and the effect of particle solubility, *Environ. Sci. Technol.*, 2006, vol. 40, pp. 4374–4381.
20. Franklin, N., Rogers, N., Apte, S., Batley, G., Gadd, G., and Casey, P., Comparative toxicity of nanoparticulate ZnO, bulk ZnO, and $ZnCl_2$ to a freshwater microalga (*Pseudokirchneriella subcapitata*): the importance of particle solubility, *Environ. Sci. Technol.*, 2007, vol. 41, pp. 8484–8490.
21. Heinlaan, M., Ivask, A., Blinova, I., Dubourguier, H.C., and Kahru A., Toxicity of nanosized and bulk ZnO, CuO and TiO_2 to bacteria *Vibrio fischeri* and crustaceans *Daphnia magna* and *Thamnocephalus platyurus, Chemosphere*, 2008, vol. 71, pp. 1308–1316.
22. Aruoja, V., Dubourguier, H.C., Kasemets, K., and Kahru, A., Toxicity of nanoparticles of ZnO, CuO and TiO_2 to microalgae *Pseudokirchneriella subcapitata, Sci. Total Environ.*, 2009, vol. 407, no. 4, pp. 1461–1468.

Translated by N. Kuznetsova